

Resonant ion-pair formation in electron collisions with HD^+ and OH^+

Å. Larson,¹ N. Djurić,² W. Zong,^{2,3} C. H. Greene,² A. E. Orel,⁶ A. Al-Khalili,³ A. M. Derkach,³ A. Le Padellec,⁴ A. Neau,³ S. Rosén,³ W. Shi,³ L. Viktor,³ H. Danared,⁵ M. af Ugglas,⁵ M. Larsson,³ and G. H. Dunn²

¹*Department of Physics, The Royal Institute of Technology (KTH), S-100 44 Stockholm, Sweden*

²*JILA and Department of Physics, University of Colorado and National Institute of Standards and Technology, Boulder, Colorado 80309-0440*

³*Department of Physics, Stockholm University, Box 6730, S-113 85 Stockholm, Sweden*

⁴*LCAR UMR 5589, Université Paul Sabatier-Toulouse III, 118 route de Narbonne, Bâtiment III R1 b4, 31062 Toulouse Cedex 4, France*

⁵*Manne Siegbahn Laboratory, S-104 05 Stockholm, Sweden*

⁶*Department of Applied Science, University of California, Davis, Livermore, California 94550*

(Received 24 February 2000; published 13 September 2000)

Resonant ion-pair formation from collisions of electrons with electronic and vibronic ground-state diatomic molecular ions has been studied in the present work for HD^+ and OH^+ . The cross section for HD^+ has a magnitude of the order of $3 \times 10^{-19} \text{ cm}^2$ and is characterized by an energy threshold and 14 resolved peaks in the energy range up to 16 eV. A theoretical study confirms that the structures derive primarily from quantum interference of the multiple dissociation pathways. Measurements for OH^+ reveal that the cross section for H^+ and O^- formation is lower than 10^{-21} cm^2 at energies of 6 and 12 eV.

PACS number(s): 34.80.Ht, 34.50.Gb, 31.50.+w

I. INTRODUCTION

The capture of an electron by a molecular ion can be stabilized by fast molecular dissociation, a process known as dissociative recombination (DR). In an ionized gas where the gas temperature is of the order of a few thousand degrees or less, and the electron temperature is lower than a few eV, DR is the dominating process leading to the removal of positive and negative charges. If a molecular ion captures an electron and dissociates into positively and negatively charged species, the process is called resonant ion-pair (RIP) formation. It can be described as



where KER is the kinetic-energy release. Although the process proceeds through the same compound state as DR, it preserves the number of positive and negative charges. While extensive experimental and theoretical investigations have been carried out on DR [1,2], RIP has received limited attention [3]. Cross sections for the formation of the ion-pair $\text{H}^- + \text{He}^+$ in electron collisions with the HeH^+ molecule have recently been calculated using propagation of wave packets on coupled potentials [4]. In experimental studies of ion-pair formation, a cross section into a well-defined asymptotic state is measured. It therefore should provide a sensitive study of doubly excited states and their decay dynamics, especially if experiments with ground state molecular ions can be performed, and hence it will pose the best challenge to theory. In RIP measurements using a storage ring and detection of negatively charged fragments, good statistical precision and excellent energy resolution characterize the results which should stand as a paradigm for the understanding of bond-breaking processes, including both dissociative recombination and resonant ion-pair formation itself.

A letter describing the first experimental study of RIP in the ion storage ring CRYRING was recently published [5]. In the present paper we describe the experiments on HD^+ and OH^+ in more detail, and present new theoretical results for HD^+ that we compare with the experimental results.

II. EXPERIMENT

The experiment was carried out with the storage ring CRYRING at the Manne Siegbahn Laboratory [6] in Stockholm. The basic experimental setup for the measurement of electron-molecular ion collisions has been described elsewhere [7]. The ions were produced in a conventional electron-impact ion source (MINIS) and injected into the ring, in the case of HD^+ after pre-acceleration by a radio frequency quadrupole accelerator to the injection energy of 300 keV/amu. Final acceleration of the circulating ion beam to the designed energy was done by a radio frequency driven drift tube [8]. The stored ion beam was merged with the electron cooler beam over a distance of 85 cm. Charged reaction products formed in the interaction region were separated from the stored ion beam in the bending magnet following the electron cooler section, and detected by a surface barrier detector (SBD). High ion beam energy is usually favored because it suppresses beam losses by collisions with residual gas molecules, thus improving the signal to noise ratio and beam lifetime. However, an energetic particle may penetrate the SBD, so that the full beam energy is not deposited in the detector, something which may affect the resolution. The beam energy of HD^+ was set to 3.5 MeV/amu for optimization. The lifetime of the beam was ≈ 7 s. For a heavy ion like OH^+ , the ions were stored at the maximum energy, which is limited by the maximum magnetic field of the bending magnets. The vacuum chamber of the dipole (bending) magnet has been modified so that a SBD can be inserted for detection of the negative fragments. The SBD

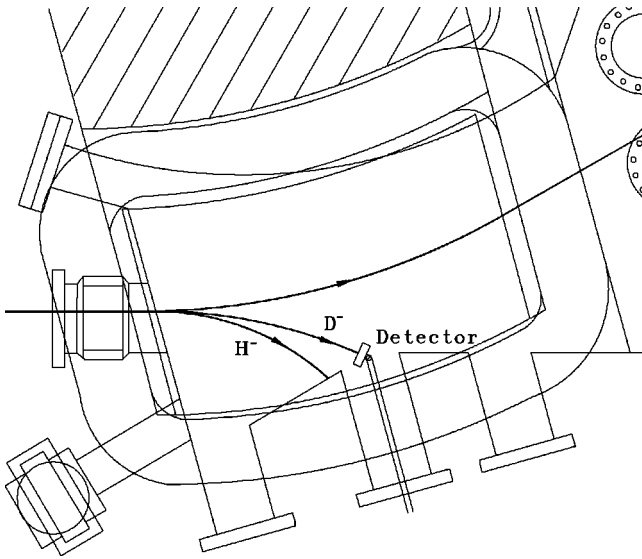


FIG. 1. The dipole chamber in CRYRING immediately following the straight section containing the electron cooler. The trajectories of the HD^+ ion beam are shown together with the trajectories that the negative ions follow. They coincide with the ion beam trajectory until they enter the magnetic field of the dipole magnet. The H^- cannot reach the detector because of the geometric limitation.

was mounted on a linear motion feed-through by which its position can be adjusted, providing the possibility of detecting negative ions with different Q/M ratios. In this measurement, however, only the heavier negative fragments were detected. The lighter H^- , due to its larger Q/M ratio, was blocked by the vacuum chamber and could not reach the detector, as can be seen in Fig. 1.

A. Measurement of HD^+ and OH^+

These measurements were performed by a “scan” method, which is similar to that used in dielectronic recombination experiments [9], that is, the interaction energy was controlled by varying the cathode voltage over a range that covered interesting RIP resonances. As shown in Fig. 2, the ion beam was first cooled for 3 seconds prior to the energy scan, allowing vibrational relaxation of the molecular ions. After the HD^+ had been translationally cooled by the electron beam, the cathode voltage was changed to its maximum value and then scanned downwards, crossing the cooling voltage, to the minimum, and then jumped back to the cooling voltage again. The total time for a voltage scan was 4 seconds and the scan covered the energy region of approximately 0–16 eV in the center-of-mass (c.m.) frame twice, once with the electron velocity higher than the ion velocity, and once with the electron velocity lower than the ion velocity. The RIP is energetically possible only when the incident electron energy exceeds a threshold, which is estimated to be approximately 1.9 eV (the difference between the dissociation energy of the ground-state ion and the electron affinity of D). A fast change of the electron cooler cathode voltage was performed over the energy region of 0–1.2 eV in order to avoid a change in the beam velocity due to the drag force

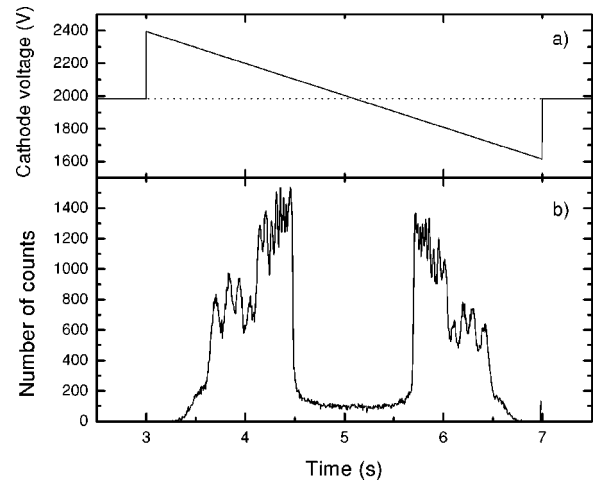


FIG. 2. (a) The figure shows how the cathode voltage of the electron cooler is scanned as a function of time during one injection. The time equal to zero represents the time when the injected ions have reached full beam energy, 3.5 MeV/amu. The ion beam is cooled by the electron beam when the velocity of the two beams is matched. This corresponds to a cathode voltage of the electron cooler of about 1.98 keV. (b) The raw data measured as a function of time. The data were accumulated during 1854 complete injection cycles.

(see Sec. II B) and the occurrence of beam heating. After each injection of new ions, the cycle was repeated. The data were taken in 1854 complete cycles. The data recorded contained two complete RIP spectra and each data set contained 3000 channels. No significant difference was observed between the two spectra measured for positive and negative relative velocities. The error associated with the data analysis can thus be checked by comparison of the two spectra.

The number of ions stored in the ring has to be measured in order to obtain absolute cross sections for RIP. It was determined from measurement of the ion beam current using an inductive current integrator. Since the decay of ion beam (during the data taking time) is non-negligible the beam current was sampled in the whole machine cycle simultaneously with the measurement, providing an averaged current spectrum. The electron beam current was 96 mA for HD^+ .

The measurement of OH^+ was performed by means of a similar protocol as for HD^+ , with the SBD positioned to detect O^- . The RIP threshold was expected to occur at 3.5 eV. Despite a careful search, no O^- ions were detected. Thus, we can only give an upper limit to the cross section for the production of $\text{O}^- + \text{H}^+$.

B. Data analysis

1. Toroidal correction

At both edges of the electron cooler, toroidal magnetic fields that are used to deflect the electron beam into and out of the interaction region add a transverse component to the guiding magnetic field. Since the electron beam follows the magnetic field, an angle thus exists between the electron and ion beams at each end of the interaction region. This results in higher collision energies as compared with parallel beams

in the cooler, hence these regions are usually excluded when defining the interaction length. However, the contributions from these parts must be taken into account, in particular in a case like HD^+ for which the cross section is zero below the threshold of 1.9 eV [10].

Figure 2 shows the raw HD^+ data recorded in this measurement. The abrupt change of rate indicates the existence of an energy threshold for the RIP process. Formation of ion pair is energetically forbidden below it. Since the molecular ions were vibrationally relaxed, the rates below the threshold revealed in the data are thus solely from the edges of the cooler where the energies exceed the threshold. The rate from charge transfer in collision with residual gas molecules is expected to be negligibly small due to its low cross section at high collision energy.

The count rate $R_m(E_d)$ recorded at the detuning energy, E_d (i.e., the relative energy between ions and electrons), can be written as

$$R_m(E_d) = S_i n_i n_e \left[\alpha(E_d) \ell + \int \alpha[E(E_d, x)] dx \right], \quad (2)$$

where S_i is the overlap area of the two beams, ℓ is the interaction length, and n_i and n_e are ion density and electron density, respectively. The interaction energy $E(E_d, x)$, as a function of detuning E_d at distance x , is calculated by using a model based on the knowledge of the toroidal field in the region. The integral that represents the toroidal effect is calculated for the region where two beams merge with an angle. The rate coefficient α at E_d can thus be expressed as

$$\alpha(E_d) = \alpha_m(E_d) - 2/\ell \int \alpha[E(E_d, x)] dx \quad (3)$$

where the factor 2 accounts for both sides of the cooler.

The correction for the toroidal effect is done by solving the equation iteratively. The measured coefficient spectrum $\alpha_m(E)$ is used as the first-order estimation of $\alpha(E)$ for calculation of the integration.

In order to make the toroidal correction, it is crucial to model the magnetic field properly and derive the energy as a function of position in this region. We assume that electrons moved along the magnetic field lines so that the interaction energy, $E(E_d, x)$, can be calculated from the ion beam energy, the detuning energy E_d and the angle between the two beams at a certain place x .

The existence of an energy threshold in RIP for HD^+ provides a check of the approach used for the toroidal correction. We varied the boundary position in our magnetic field model until the rate coefficient derived from the equation became zero below the threshold.

2. Drag force

When the average electron and ion velocities differ, the interaction between them tends to reduce the difference. The net effect is a drag force acting on the ions, accelerating them towards the electron velocity in the case where the electrons initially move faster than the ions.

The drag force can be written, nonrelativistically and without inclusion of magnetic effects arising from the weak solenoidal field that guides the electron beam, as [11]

$$\mathbf{F}(t) = F_o c^2 \int L_c(\mathbf{v}_e, \mathbf{v}_i) f(\mathbf{v}_e) \frac{\mathbf{v}_e - \mathbf{v}_i}{|\mathbf{v}_e - \mathbf{v}_i|^3} d^3 v_e, \quad (4)$$

where $F_o = 4\pi Q^2 n_e r_e m_e c^2$, and Q is the ion charge, r_e is the classical electron radius, n_e is the electron density, \mathbf{v}_i is the average ion velocity, \mathbf{v}_e is the electron velocity, $f(\mathbf{v}_e)$ is a flattened Maxwellian velocity distribution [12] of the electron beam, and L_C is the so called Coulomb logarithm for the ion-electron collisions (a dimensionless parameter on the order of 10).

Affected by the drag force, the ion velocity tends to vary during a scan of the electron energy in a measurement. This effect becomes important for higher charge states, light ions, and, most importantly, when the velocity difference is small.

The variation of the ion energy due to the drag force can be modeled, via the corresponding velocity, by the differential equation

$$\frac{dv_i}{dt} = \frac{\eta}{M_i} \frac{\ell}{L_r} F_z(t), \quad (5)$$

where M_i is the ion mass, $F_z(t)$ is the longitudinal component of the drag force, ℓ is length of the interaction region, and L_r is the circumference of the ring. The ratio ℓ/L_r represents the fraction of time over which the force is applied as the ions circulate in the ring. η is a free parameter that compensates for the errors from the uncertainties in beam temperatures and the interaction length.

Solving Eq. (5) numerically yields the real ion energy at each scan point. The correct interaction energy can thus be derived [13].

In this experiment, however, the correction for the drag force effect was performed without solving the differential Eq. (5). The following approach was used instead. The drag force decreases rapidly with increasing relative velocity. As a result, its effect on the ion beam energy is important only at low interaction energies, say, less than 1 eV, and becomes negligible at higher interaction energies. In other words, the ion energy changes due to the drag force only at the energy region below 1 eV and is constant above that. Because of the energy threshold of the RIP process being about 1.9 eV for HD^+ , the ion energy at the interaction energy range related to RIP can be regarded as constant. The effect of the drag force on the ion energy can be regarded as causing a shift of the ion beam energy from its value at cooling.

III. EXPERIMENTAL RESULTS

A. Results from measurement on HD^+

The measured absolute cross section for D^- production from the RIP of HD^+ is shown in Fig. 3. The data were corrected according to the procedures described in the previous section and were essentially identical whether electrons were slower or faster than the ions. Thus, the data have been combined, during several separate runs. The cross section

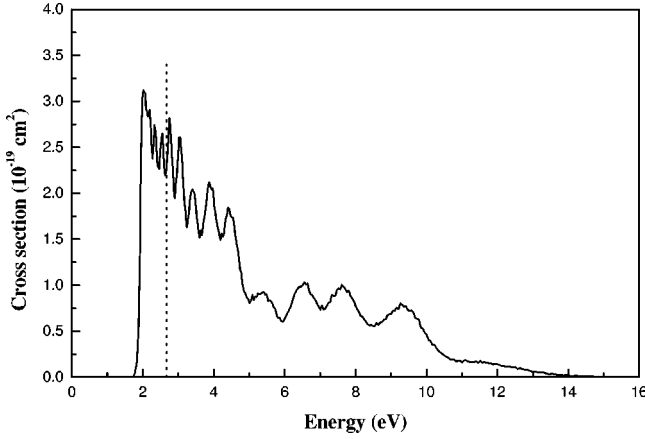


FIG. 3. The experimental cross section for $\text{HD}^+ + e^- \rightarrow \text{H}^+ + \text{D}^-$ as a function of electron energy. The vertical dotted line shows the dissociation energy of the HD^+ molecule. Peaks situated above this line cannot be explained by indirect resonant capture into the Rydberg state potentials below the ionic ground state.

risers sharply at 1.92 eV (half-rise position), which is very close to the expected position at 1.913 eV. Figure 4 shows the energetics. The region between the threshold for ion-pair formation and the dissociation energy of HD^+ at 2.667 eV is labeled Δ_1 . The first five peaks in the RIP cross section occur in this energy interval with spacings of the order of 0.2 eV. This is close to the vibrational spacing in HD^+ and initially led us to believe that the peak structure derived from vibrational excitation and resonant capture into high vibrational levels of bound Rydberg states of HD, which converge to the ground ionic state. However, this attempt to explain peaks 1–5 breaks down for peaks 6–14, and an alternative explanation was suggested in Ref. [5]. We develop a more quantitative description in Sec. IV below. The peak magnitude of the cross section is $3 \times 10^{-19} \text{ cm}^2$, and this is only a few percent of the total DR cross section (10^{-17} cm^2).

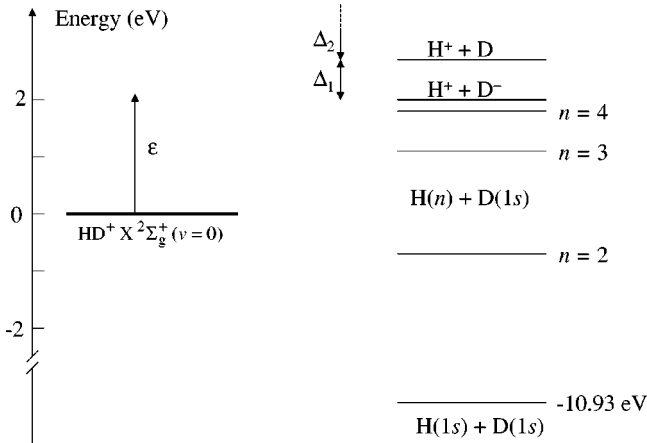


FIG. 4. Energy-level diagram for HD and HD^+ , with the zero chosen to coincide with the energy of $\text{HD}^+ X^2\Sigma_g^+(v=0)$. The ion-pair limit is located just above $\text{H}(n=4) + \text{D}(1s)$. The energy region labeled Δ_1 is located between the ion-pair limit and the dissociation limit of HD^+ .

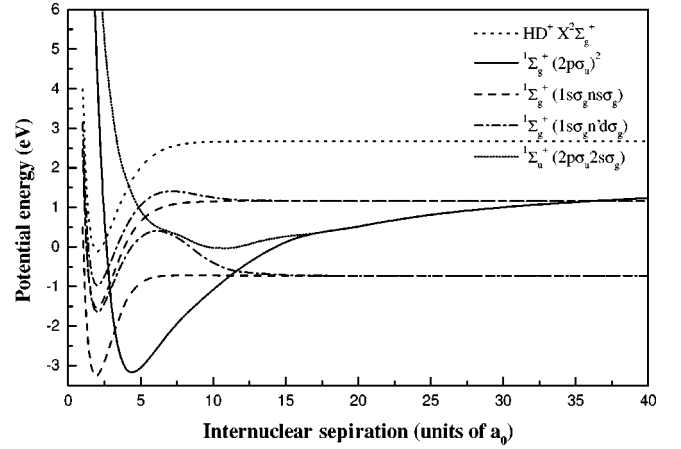


FIG. 5. Some of the relevant diabatic potentials of the HD^+ and HD molecules. The ground state of the HD^+ ion, $X^2\Sigma_g^+$ is shown as a dotted line. Since we start with the molecular ions in the vibrational ground state $v=0$, the energy scale is relative to this level. The most important dissociative state of the HD molecule is the $1\Sigma_g^+(2p\sigma_u)^2$, which correlates with the ion-pair channel at infinity. This diabatic state crosses the neutral $1\Sigma_g^+$ Rydberg states located below the ionic ground state. Nondiabatic transitions occur, the most important of which are from the ion-pair state into the Rydberg states dissociating into the $\text{H}(n=2) + \text{D}$ and $\text{H}(n=3) + \text{D}$ limits. Another important pathway in the energy range from 5 eV to 10 eV is the doubly-excited $1\Sigma_u^+(2p\sigma_u 2s\sigma_g)$ state, which is shown diabatically out to $R \approx 5$ a.u. and then adiabatically to large R .

B. Results from measurement on OH^+

The absence of production of O^- ions when OH^+ was used as a target ion makes it possible only to determine an upper limit for the cross section. Thus, at 6 eV and 12 eV the cross section for formation of H^+ and O^- is smaller than 10^{-21} cm^2 .

IV. THEORETICAL TREATMENT OF HD^+

In the measured cross section for ion-pair formation in electronic recombination with HD^+ , 14 well-resolved peaks are observed. In DR, peaks in the cross section are sometimes observed, and they are often explained by capture into vibrationally excited Rydberg states that subsequently predissociate into neutral fragments (this is usually called the indirect process [14]). However, as mentioned above, this process is not possible for electron collision energies above the dissociation limit of the molecular ion. The dissociation energy of HD^+ is 2.667 eV. Five of the peaks observed in the measured cross section are situated below this threshold and the remaining peaks are above this limit. The peaks that are above the dissociation limit cannot be explained by the indirect process. A Franck-Condon analysis showed [5] that these peaks cannot be entirely explained by capture into higher excited neutral dissociative states. The peaks must be explained by another type of mechanism.

Figure 5 shows some of the relevant diabatic potential curves of the HD^+ and HD molecules [15]. The ground state potential $X^2\Sigma_g^+$ of the molecular ion is included in the figure as a dotted line. The lowest neutral $1\Sigma_g^+$ dissociative

state of HD is shown in the figure. At small internuclear separations this state is dominated by the configuration $(2p\sigma_u)^2$. Diabatically, the state correlates with the ion-pair limit, $H^+ + D^-$, at infinity. Below the ionic ground state there are series of Rydberg state potentials. The most important [16] are the $^1\Sigma_g^+(1s\sigma_g n s\sigma_g)$ and the $^1\Sigma_g^+(1s\sigma_g(n+1)d\sigma_g)$ Rydberg states, approaching the $H + D(n)$ limit asymptotically.

In a diabatic representation, the $^1\Sigma_g^+(2p\sigma_u)^2$ ion-pair state crosses many of these Rydberg state potentials twice, both at small and large internuclear separations. These are the Rydberg states associated with the $H(n=2) + D(1s)$ and $H(n=3) + D(1s)$ limits. Since the states are of the same symmetry, they will be coupled by the electronic part of the Hamiltonian (diabatic coupling). The ion-pair state crosses the potentials going to the $H(n=4) + D(1s)$ limit at very large internuclear separation ($R = 230 a_0$). The electronic coupling between the states at this large internuclear separation can be neglected. These couplings will induce different pathways to the ion-pair limit. The dissociating wave can either diabatically follow the dissociative $^1\Sigma_g^+(2p\sigma_u)^2$ state to the ion-pair limit, or it can make a transition to one of the Rydberg state potentials, propagate along the Rydberg potential until it reaches the second curve crossing and there make a transition back to the ion-pair state. It will be shown here that the quantum interference between the competing pathways is the dominant mechanism for producing the peaks observed in the measured ion-pair cross section.

In the present calculation, six states have been included. These are the lowest resonant $^1\Sigma_g^+(2p\sigma_u)^2$ state, the two Rydberg states $[(1s\sigma_g 2s\sigma_g)$ and $(1s\sigma_g 3d\sigma_g)]$ associated with the $H(n=2) + D(1s)$ limit, and the lowest Rydberg state $(1s\sigma_g 3s\sigma_g)$ associated with the $H(n=3) + D(1s)$ limit. For electron collision energies above approximately 6 eV, the doubly-excited $^1\Sigma_g^+(2p\sigma_u)^2$ state cannot by itself describe the dissociation dynamics adequately. Higher excited neutral repulsive states become important. Included in the calculation are the lowest $^1\Sigma_u^+$, $(2p\sigma_u 2s\sigma_g)$ resonant state [17] and the second $^1\Sigma_g^+$ state, $(2p\sigma_u 3p\sigma_u)$ [15].

The transition amplitudes at each individual crossing are treated using the Landau-Zener model [18]. According to this model, the probability of a transition between two diabatic states is given by

$$P_{ij}(E) = 1 - \exp\left[-\frac{2\pi c_{ij}^2}{\alpha v}\right], \quad (6)$$

where c_{ij} is the electronic coupling matrix element between states i and j . The absolute slope difference between the potentials is denoted α , while v is the relative velocity of the fragments; all these quantities are evaluated at the curve crossing point and are in atomic units.

For each curve crossing at small R , we approximate the electronic coupling matrix element connecting any given diabatic potential curve to the dissociative state by one-half of the closest energy separation between the two relevant *adiabatic* potentials. Our calculations suggest that the $(1s\sigma_g n s\sigma_g)$ Rydberg states are coupled more strongly to the

lowest $^1\Sigma_g^+$ dissociative state than are the $(1s\sigma_g n d\sigma_g)$ Rydberg states, at least in the range $R \approx 3-4$ a.u.

At large R , we adopt the coupling matrix elements of Sidis *et al.* [19]. A number of potential energy curves are correlated with the asymptotic limit $H(n) + D(1s)$. If fine structure can be ignored, then the Σ potential curves, for instance, possess an n -fold degeneracy at $R \rightarrow \infty$. The potential energy curve of the Σ ion-pair state crosses these n potential curves at a very large distance ($R_x = 11.2 a_0$ for $n = 2$ and $R_x = 35.6 a_0$ for $n = 3$), where the hydrogenic potential curves are almost degenerate. Lewis [20] has shown that only one linear combination of the n degenerate states couples to the ion-pair state. We have carried out a series of calculations to estimate the couplings between these states. These calculations of the adiabatic $^1\Sigma_g^+$ excited state potential energy curves indicate that $(1s\sigma_g 3d\sigma_g)$ and $(1s\sigma_g 3s\sigma_g)$ are the approximate designations of the coupled states that correlate respectively with the $H(n=2) + D$ and $H(n=3) + D$ limits. Details of these calculations will be published elsewhere [21].

The quantum interference effects are primarily controlled by the energy-dependent phases accumulated along the different pathways. The semiclassical phase in the WKB approximation is given by

$$\varphi_j(E) = \int_{R_E}^{R_{\text{final}}} k_j(R) dR = \int_{R_E}^{R_{\text{final}}} \sqrt{2\mu(E - V_j(R))} dR. \quad (7)$$

Here R_E is the appropriate Condon point, namely the internuclear separation distance where the initial excitation step in a Born-Oppenheimer approximation equals the collision energy E . Autoionization from the resonant state is treated by including half of the autoionization width $\Gamma(R)$ as a complex term of the potential for internuclear distances smaller than the crossing point of the dissociative HD potential curves and the ionic ground state potential. The dissociation amplitudes, $A_j(E)$, for the different pathways j are reduced somewhat by the loss of flux into the infinite number of Rydberg states whose dissociation limits lie energetically above the ion-pair threshold. In the ‘‘projection approximation’’ the initial capture probability, P_{cap} , is estimated using a delta function for the nuclear wave function of the dissociative state [22]. The probability of dissociating into the channel $H^+ + D^-$ is assumed to equal the probability of dissociation into $H^- + D^+$. Since only the D^- fragments were detected in the experiment, this probability must be estimated. The total amplitude for dissociation into the ion-pair state is a coherent sum of the amplitudes for the competing indistinguishable pathways and the cross section for ion-pair formation becomes

$$\sigma_{ip}(E) = \frac{2\pi^3}{E} P_{\text{cap}}(E) \left| \sum_j A_j(E) \exp[i\varphi_j(E)] \right|^2. \quad (8)$$

The cross section that results from this calculation is shown in Fig. 6. In the calculation, the contribution from the lowest $^1\Sigma_u^+$ state is included incoherently, because it derives almost exclusively from the $l = 1$ partial wave of the incident

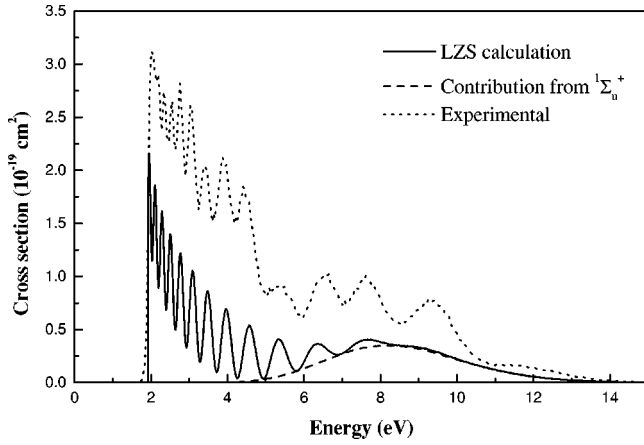


FIG. 6. Cross section for D^- formation in electron collisions with $HD^+(v=0)$, calculated using a time-independent Landau-Zener-Stückelberg model. The transition probabilities at the curve crossings are estimated using the Landau-Zener formula. Here the quantum interference between the different dissociation pathways is included. As the figure indicates, the incoherent contribution from the lowest $^1\Sigma_u^+(2p\sigma_u 2s\sigma_g)$ state is important for energies above 5 eV. The dotted curve represents the measured cross section, as shown in Fig. 3.

electron and thus leads to a distinguishable final ion-pair state with nonzero angular momentum and odd total parity. The second $^1\Sigma_g^+$ resonant state correlates diabatically with $H(n=3)+D$ and crosses the ion-pair state around $R = 35.6 a_0$. In the present calculation it is assumed to be one of the inactive states, not strongly coupled to the ion-pair state.

The peaks obtained in the calculated cross section in Fig. 6 originate from the interference effects from the indistinguishable competing dissociation paths. If the cross section is calculated instead by *incoherently* adding the flux contributions that lead to the ion-pair dissociation,

$$\sigma_{ip}(E) = \frac{2\pi^3}{E} P_{\text{cap}}(E) \sum_j |A_j(E) \exp[i\varphi_j(E)]|^2, \quad (9)$$

no peaks are observed, as can be seen in Fig. 7. However, it exhibits reasonably good agreement with the measured cross section in its overall magnitude and shape.

V. DISCUSSION

The absence of an O^- signal when OH^+ is used as target ion makes it impossible to determine a cross section for ion-pair formation. It is only possible to infer that cross section is smaller than 10^{-21} cm^2 at electron energies 6 and 12 eV. It is difficult to establish why there is an absence of a signal, but some qualitative arguments can be put forward. Figure 8 shows an energy-level diagram for OH and OH^+ and some of the atomic limits. It is well known that dissociative recombination of OH^+ occurs primarily through the $2^2\Pi$ state of OH [23,24]. This state correlates with the $O(^1D)+H(n=1)$ limit, as can be seen in Fig. 8. It was shown that when the electron energy is sufficient to open the $O(^3P)+H(n=1)$

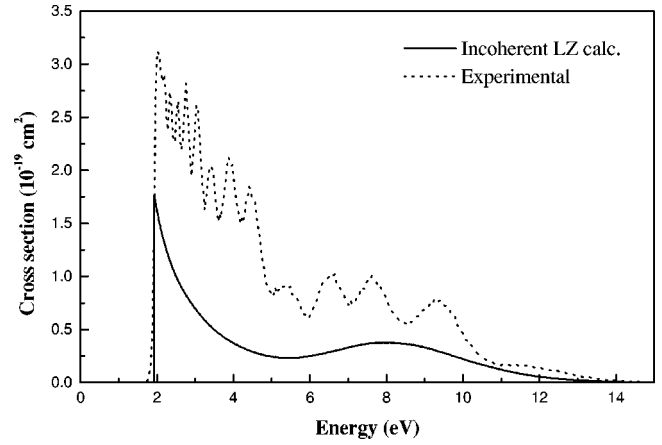


FIG. 7. The solid curve is the cross section for D^- formation in electron collisions with $HD^+(v=0)$, calculated using an incoherent sum of fluxes going to the ion-pair limit. Since the interference effects from the competing dissociation paths are not treated, no peaks are obtained in the calculated cross section. For comparison, the measured experimental cross section is included in the figure as the dotted curve.

$=2)$ limit, a fraction of the dissociating flux will be redirected to this limit by adiabatically following any of the $3^2\Pi$, $4^2\Pi$, and $5^2\Pi$ states [25], which have been calculated theoretically by Van Dishoek and Dalgarno [26]. This redirection appears to occur over only a limited interval of electron energies, from threshold at 1.64 to about 2.5 eV. Thus, at 3.5 eV, which is the threshold for ion-pair formation, there is no flux redirected through the $3^2\Pi$, $4^2\Pi$, and $5^2\Pi$ states, and it seems very unlikely that the outgoing flux somehow should reach the $2^2\Pi$ state dissociating to $O^- + H^+$. When the electron energy is increased significantly above the threshold for ion-pair formation, it is not inconceivable that the $2^2\Sigma^+$ and $2^2\Pi$ states correlating with the ion-pair limit could be favorably located for an electron capture process from the OH^+ ground state. In the absence of any theoretical calculations of these states, however, this statement remains a speculation, which the experimental results do not corroborate.

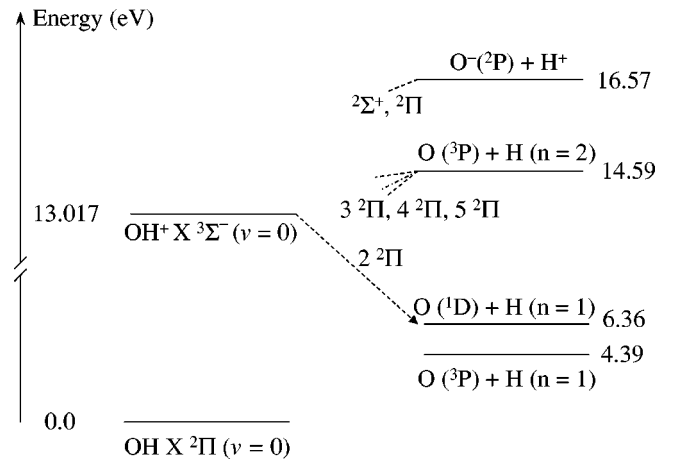


FIG. 8. Energy-level diagram for OH and OH^+ . The zero-point energy is defined as $OH X ^2\Pi(v=0)$.

The only previous measurement of electron collision-induced ion-pair formation in a diatomic system was an inclined beams experiment with H_2^+ [27]. A meaningful comparison with the present work is not possible since H_2^+ ions populating all 19 vibrational levels were used [27]. Neither an interference pattern nor an energy threshold was observed, and the RIP cross section was more than an order of magnitude larger than measured for $\text{HD}^+(v=0)$ in the present work. Ion-pair formation induced by photoabsorption of HD has also been studied [28]. The relative photo-induced cross section was measured from threshold at 714 Å over a photon energy range of about 0.4 eV. The ratio of H^-/D^- was found to be about 2 just above threshold. The ratio decreased with increasing photon energy, but this was at least partly ascribed to the decreasing detection efficiency of H^- [28]. This aspect of RIP could not be tested in the present work, unfortunately, because of the inaccessibility of H^- (see Fig. 1). Our theoretical model assumed that both the gerade and ungerade pathways produced H^- and D^- in equal amounts.

Recently, a study of ion-pair formation in VUV photoabsorption experiments of H_2 and D_2 , has shown peaks in the measured cross section [29]. The structure in the cross section has also been interpreted by this group as evidence of quantum interference effects in the dissociation dynamics.

A time-independent Landau-Zener-Stückelberg calculation, which in contrast to the Landau-Zener model also includes the phase, confirms that the peaks observed in the measured cross section of ion-pair formation in HD^+ originate from the interference of different pathways leading to the ion-pair limit. The resulting energy-dependent phases produce maxima and minima in the cross section when the product amplitudes are added coherently. The calculation shows that the dominant interfering pathways are the dissociative $1\Sigma_g^+(2p\sigma_u)^2$ state and the $5^1\Sigma_g^+$ state that approaches the $\text{H}(n=3)+\text{D}(1s)$ limit asymptotically. The shape and magnitude of the calculated energy-dependent cross section are both extremely sensitive to the details of the electronic coupling matrix elements between these diabatic potential curves. The Landau-Zener model has limited applicability to the present situation, since it is a model only for a curve crossing between two isolated states. In fact, both the small- R and large- R crossings in this system involve multiple potential curves, and these curve crossings are not sufficiently well separated to invoke the two-state model accurately.

Despite the limitations of Landau-Zener-Stückelberg-type models, reasonably good agreement has been obtained between our model calculations and the measured ion-pair formation cross section caused by an electron collision with HD^+ . This agreement is fairly good in the positions of the interference maxima and also in the overall cross section

magnitude. It should be pointed out, however, that the channel couplings used in existing diabatic Hamiltonians for HD had to be adjusted somewhat, in order to achieve this modest level of agreement with experiment. This is presumably because previous experiments and potential curve calculations that were incorporated into the determination of these diabatic Hamiltonians simply had insufficient information to identify a unique set of couplings. The great sensitivity of the interference pattern observed in this RIP experiment should ultimately help to determine an improved diabatic Hamiltonian which has far less nonuniqueness. These issues will be discussed in greater detail elsewhere.

A number of possibilities might be responsible for the residual discrepancies between theory and experiment. For one thing, we use a relatively simple model for the dissociation dynamics. For instance, the present study includes only states of 1Σ symmetry, since this is the symmetry of the ion-pair state at small R . However, when the spin-orbit coupling at large separations is considered, states of 3Σ and Π symmetries might also play a role in the ion-pair formation. As another example, while we incorporate the loss of flux from the doubly-excited states into high Rydberg states in our model, we have not included the possibility that some fraction of that flux could be redirected back to the ion-pair state through various pathways. This type of redirection is included in the calculations only for the lowest Rydberg states, with $n < 4$. In summary, the simple Landau-Zener-Stückelberg model implemented in this paper has shown conclusively that the observed peaks in the measured D^- RIP cross section are caused by a quantum mechanical interference. Nevertheless, an improved quantitative description of resonant ion-pair formation in e- HD^+ collisions remains an important goal for future studies.

ACKNOWLEDGMENTS

The authors would like to thank the staff of the Manne Siegbahn Laboratory for their assistance in this experiment. We are also grateful to Ioan Schneider, Annick Suzor-Weiner and Xavier Urbain for fruitful discussions. This work was supported by the Swedish Foundation for International Cooperation in Research and Higher Education (STINT), the Göran Gustafsson Foundation, and the Swedish Natural Science Research Council. G.D. and N.D. were supported in part by the US Department of Energy, Fusion Energy Branch under Contract No. DE-A102-95ER54294. The work of C.H.G. has been supported in part by the Department of Energy, Office of Basic Energy Sciences. A.E.O. was supported by the National Science Foundation, Grant No. PHY-97-22136 and some work was performed under the auspices of the U.S. Department of Energy by University of California Lawrence Livermore National Laboratory under Contract No. W-7405-Eng-48.

[1] M. Larsson, *Annu. Rev. Phys. Chem.* **48**, 151 (1997).

[2] M. Larsson, *Dissociative Electron-Ion Recombination Studies Using Ion Synchrotrons*, Adv. Ser. Phys. Chem. Vol. 10: Photoionization and Photodetachment, edited by C. -Y. Ng

(World Scientific, Singapore, 2000), p. 693.

[3] G. H. Dunn and N. Durić, in *Novel Aspects of Electron-Molecule Scattering*, edited by K. Becker (World Scientific, Singapore, 1998), p. 241.

- [4] Å. Larson and A. E. Orel, *Phys. Rev. A* **59**, 3601 (1999).
- [5] W. Zong, G. H. Dunn, N. Durić, M. Larsson, C. H. Greene, A. Al-Khalili, A. Neau, A. M. Derkatch, L. Viktor, W. Shi, A. Le Padellec, S. Rosén, H. Danared, and M. af Ugglas, *Phys. Rev. Lett.* **83**, 951 (1999).
- [6] K. Abrahamsson *et al.*, *Nucl. Instrum. Methods Phys. Res. B* **79**, 269 (1993).
- [7] C. Strömholm, J. Semaniak, S. Rosén, H. Danared, S. Datz, W. van der Zande, and M. Larsson, *Phys. Rev. A* **54**, 3086 (1996).
- [8] K. Abrahamsson, G. Andler, and C. B. Bigham, *Nucl. Instrum. Methods Phys. Res. B* **31**, 475 (1988).
- [9] D. R. DeWitt, R. Schuch, T. Quinteros, H. Gao, W. Zong, H. Danared, M. Pajek, and N. R. Badnell, *Phys. Rev. A* **50**, 1257 (1994).
- [10] A. Lampert, A. Wolf, D. Habs, J. Kenntner, G. Kilgus, D. Schwalm, M. S. Pindzola, and N. R. Badnell, *Phys. Rev. A* **53**, 1413 (1996).
- [11] D. R. DeWitt, R. Schuch, W. Zong, H. Gao, S. Asp, C. Biedermann, M. H. Chen, and N. R. Badnell, *Phys. Rev. A* **53**, 2327 (1994).
- [12] H. Danared, *Phys. Scr.* **T59**, 121 (1995).
- [13] D. R. DeWitt, R. Schuch, W. Zong, S. Asp, H. Gao, C. Biedermann, L. Liljeby, E. Beebe, and A. Pikin, *Phys. Scr.* **T71**, 96 (1997).
- [14] J. N. Bardley, *J. Phys. B* **1**, 365 (1968).
- [15] I. F. Schneider, O. Dulieu, and A. Giusti-Suzor, *J. Phys. B* **24**, L289 (1991).
- [16] A. Giusti-Suzor, J. N. Bardsley, and C. Derkits, *Phys. Rev. A* **28**, 682 (1983).
- [17] C. H. Greene and B. Yoo, *J. Phys. Chem.* **99**, 1711 (1995).
- [18] C. Zener, *Proc. R. Soc. London, Ser. A* **137**, 696 (1932).
- [19] V. Sidis, C. Kubach, and D. Fussen, *Phys. Rev. A* **27**, 2431 (1983).
- [20] J. T. Lewis, *Proc. Phys. Soc., London, Sect. A* **68**, 632 (1955).
- [21] A. E. Orel and Å. Larson (unpublished).
- [22] T. F. O'Malley, *Phys. Rev.* **150**, 14 (1966).
- [23] S. L. Guberman, *J. Chem. Phys.* **102**, 1699 (1995).
- [24] Z. Amitay, D. Zaffman, P. Forck, T. Heupel, M. Grieser, D. Habs, R. Repnow, D. Schwalm, A. Wolf, and S. L. Guberman, *Phys. Rev. A* **53**, R644 (1996).
- [25] C. Strömholm, H. Danared, Å. Larson, M. Larsson, C. Marian, S. Rosén, B. Schimmelpfenning, I. F. Schneider, J. Semaniak, A. Suzor-Weiner, U. Wahlgren, and W. J. van der Zande, *J. Phys. B* **30**, 4919 (1997).
- [26] E. Van Dishoek and A. Dalgarno, *J. Chem. Phys.* **79**, 873 (1983).
- [27] B. Peart and K. T. Dolder, *J. Phys. B* **8**, 1570 (1975).
- [28] W. A. Chupka, P. M. Dehmer, and W. T. Jivery, *J. Chem. Phys.* **63**, 3929 (1975).
- [29] A. M. Sands, R. A. Mackie, R. Browning, K. F. Dunn, and C. J. Latimer (unpublished).